Neuron, Volume *78*

Supplemental Information

Three Mechanisms Assemble

Central Nervous System Nodes of Ranvier

Keiichiro Susuki, Kae-Jiun Chang, Daniel R. Zollinger, Yanhong Liu, Yasuhiro Ogawa, Yael Eshed-Eisenbach, María T. Dours-Zimmermann, Juan A. Oses-Prieto, Alma L. Burlingame, Constanze I. Seidenbecher, Dieter R. Zimmermann, Toshitaka Oohashi, Elior Peles, and Matthew N. Rasband

Figure S1

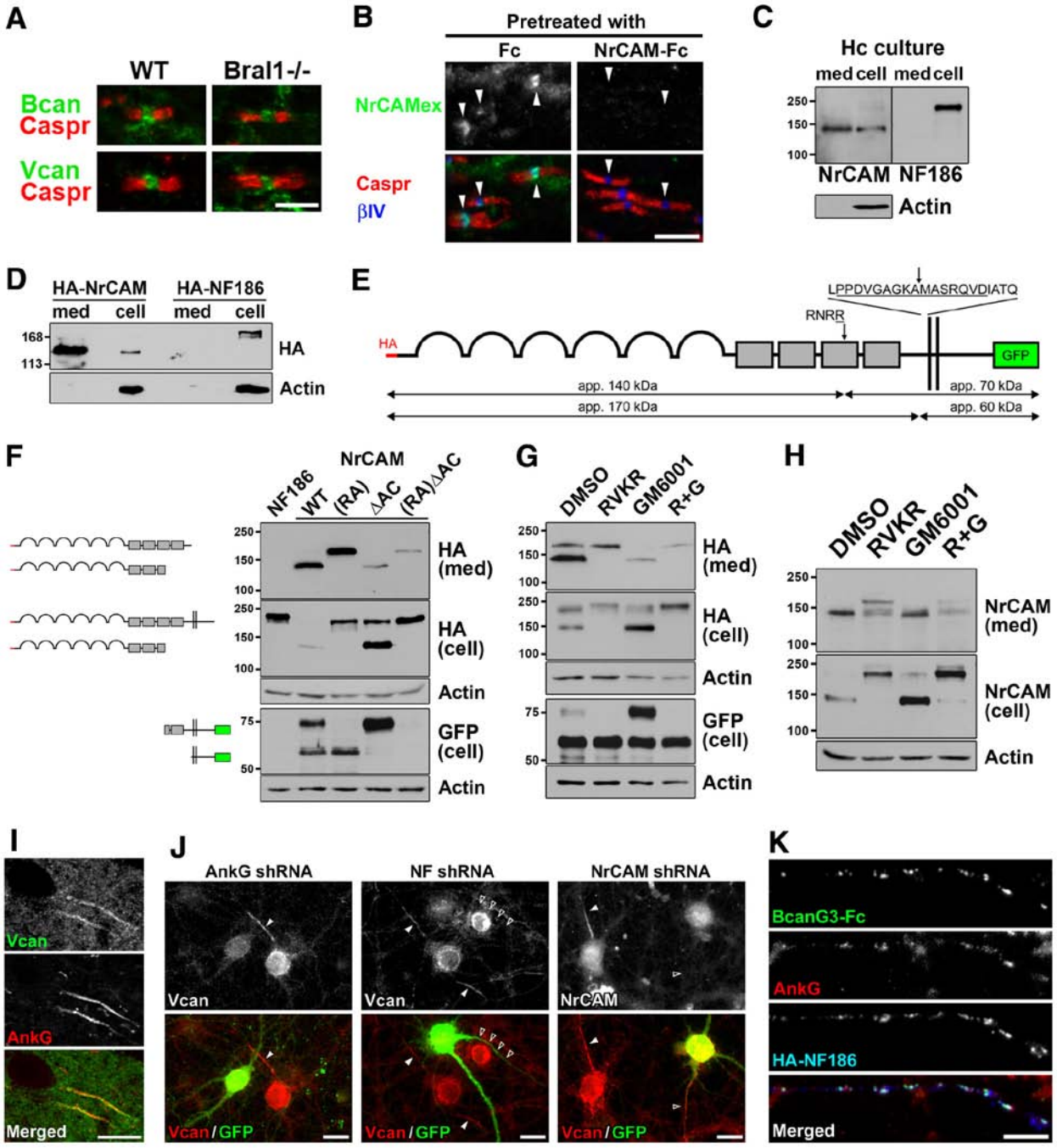
A
WT
Bral1-/-
Bcan
Caspr
Vcan
Caspr
B
Pretreated with
Fc
NrCAM-Fc
NrCAMex
Caspr
βIV
C
Hc culture
med cell med cell
250
150
100
NrCAM NF186
Actin
D
HA-NrCAM
HA-NF186
med cell med cell
168
113
HA
Actin
E
LPPDVGAGKAMASRQVDIATQ
RNRR
HA
GFP
app. 140 kDa
app. 170 kDa
app. 70 kDa
app. 60 kDa
F
NrCAM
NF186
WT
(RA)
ΔAC
(RA)ΔAC
250
150
100
HA (med)
HA (cell)
Actin
75
50
GFP (cell)
Actin
G
DMSO
RVKR
GM6001
R+G
HA (med)
HA (cell)
Actin
GFP (cell)
Actin
H
DMSO
RVKR
GM6001
R+G
NrCAM (med)
NrCAM (cell)
Actin
I
Vcan
AnkG
Merged
J
AnkG shRNA
NF shRNA
NrCAM shRNA
Vcan
Vcan
NrCAM
Vcan/GFP
Vcan/GFP
Vcan/GFP
K
BcanG3-Fc
AnkG
HA-NF186
Merged

Figure S1 Legend

Molecular composition of the ECM surrounding CNS nodes, related to Figure 2.

(A) Staining of P18 wild-type (WT) and Bral1-KO spinal cords with Bcan or Vcan (green) and Caspr (red) antibodies. Scale bar = 5 μm.

(B) NrCAM immunolabeling of adult mouse optic nerves (stained for anti-Caspr (red), anti-βIV spectrin (blue) and anti-NrCAM extracellular domain (green) antibodies) could be blocked by pre-adsorption with NrCAM-Fc, but not Fc alone. Scale bar = 5 μm. Because the anti-NrCAM intracellular domain antibody could not stain CNS nodes (Zonta et al., 2008), these together suggest NrCAM may be present in a soluble form containing only its extracellular domain at CNS nodes.

(C) Secreted NrCAM, but not NF186, is present in the media (med) collected from hippocampal neuron (Hc) cultures at 27 DIV. Med and cells (cell) were analyzed by immunoblotting with antibodies against the extracellular domains of NrCAM and NF186, or actin.

(D) To understand how NrCAM is shed from cells, and clustered at CNS nodes, we expressed full-length NrCAM or NF186 in COS-7 cells and found only NrCAM in the medium suggesting a proteolytic cleavage event of full-length NrCAM, but not NF186. The media (med) and cells (cell) collected from COS-7 cells expressing extracellularly HA-tagged NrCAM or NF186 were analyzed by immunoblotting with antibodies against HA or actin.

(E) Cartoon illustrating putative NrCAM cleavage sites (arrows) and interpretation of the cleavage products with apparent (app.) molecular weights (see **F**-**H**). The NrCAM constructs used here were either extracellularly HA-tagged or intracellularly GFP-tagged. The arcs represent the Ig domains, the grey rectangles the fibronectin III (FN III) domains and the two vertical lines the plasma membrane. The underlined R of RNRR is mutated to A in RA mutants.

The underlined 16 amino acid residue (aa) close to the transmembrane domain are deleted in ΔAC mutants. ATQ are the last three aa of the extracellular domain.

(F-H) We mutated the consensus furin cleavage site (RNRR in rat NrCAM to RNRA) in the third FN III domain (Davis et al., 1996; Kayyem et al., 1992) to determine if furin is responsible for NrCAM secretion as it is for secretion of gliomedin in the PNS (Eshed et al., 2007). The RA mutant failed to inhibit secretion of NrCAM. Instead, the size of the secreted species increased (**E** and **F**), suggesting the existence of another cleavage event closer to the transmembrane domain. Treatment with the furin inhibitor dec-RVKR-CMK showed similar changes **(G)**. To identify the second cleavage site, the 170-kDa product of the RA mutant was purified and subjected to sequencing by mass spectrometry. With this approach, we identified a second cleavage site 11 aa N-terminal to the transmembrane domain **(E)**, reminiscent of juxtamembrane cleavage by the ADAM (A Disintegrin And Metalloprotease) family of metalloproteases (Seals and Courtneidge, 2003; White, 2003). Consistent with this idea, treatment of COS-7 cells expressing wild-type NrCAM with the metalloprotease inhibitor GM6001 decreased the 170-kDa secreted product and increased the 70-kDa GFP-tagged membrane-bound fragment **(G).** The cleavage by furin was not affected by GM6001; however, the release of the 140-kDa furin cleavage product was significantly inhibited and this product was retained with the cell **(G).** To genetically block cleavage by ADAMs, we deleted 16 aa around the second cleavage site (ΔAC) in the RA mutant and found the cleavage and secretion were significantly inhibited and full-length NrCAM was highly accumulated and retained on the cells **(F).** Furthermore, the ΔAC mutation alone inhibited the production of the 60-kDa GFP-tagged membrane-bound fragment and release of the furin-cleaved product **(F)**, consistent with the treatment of WT NrCAM with GM6001 **(G)**. These data suggest that NrCAM cleavage at the ADAM site regulates shedding of

the furin-cleaved product from the surface of cells. Inhibition of furin and metalloproteases in hippocampal neuron cultures showed similar changes as in the case of COS-7 cells **(H).** These data show that NrCAM's extracellular domain is cleaved by furin, shed by ADAMs and enriched at the CNS nodal ECM. In **(F)** the media (med) and cells (cell) collected from COS-7 cells expressing HA-NF186, wild-type or mutant HA-NrCAM, NF186-GFP, or wild-type or mutant NrCAM-GFP were analyzed by immunoblotting with antibodies against HA, GFP or actin. In **(G)** the media and cells collected from COS-7 cells expressing wild-type HA-NrCAM or NrCAM-GFP and treated with DMSO, dec-RVKR-CMK (RVKR), GM6001 or both (R+G) were analyzed by immunoblotting with antibodies against HA, GFP or actin. In **(H)** the media and cells collected from hippocampal neuron cultures treated with DMSO, dec-RVKR-CMK (RVKR), GM6001 or both (R+G) were analyzed by immunoblotting with antibodies against the extracellular domain of NrCAM, or actin.

(I) Immunostaining showing axon initial segments (labeled with ankG, red) of postnatal day 24 rat cortical neurons were enriched with Vcan (green). Scale bar = 20 μm.

(J) Cultured hippocampal neurons were transfected with shRNA and GFP-expressing plasmids 3 hr after plating and immunostained at 19 DIV for Vcan (red) and ankG, NF186 (not shown) or NrCAM (the gray-scale image) to confirm efficient knockdown. Solid and open triangles point to the AIS of untransfected and transfected neurons, respectively. Scale bars = 20 μm.

(K) Purified DRG neurons were transfected with HA-NF186, incubated with preclustered BcanG3-Fc (green) and cultured for two more days before immunostaining with anti-ankG (red) and anti-HA (blue) antibodies. Scale bar = 5 μm.

Figure S2

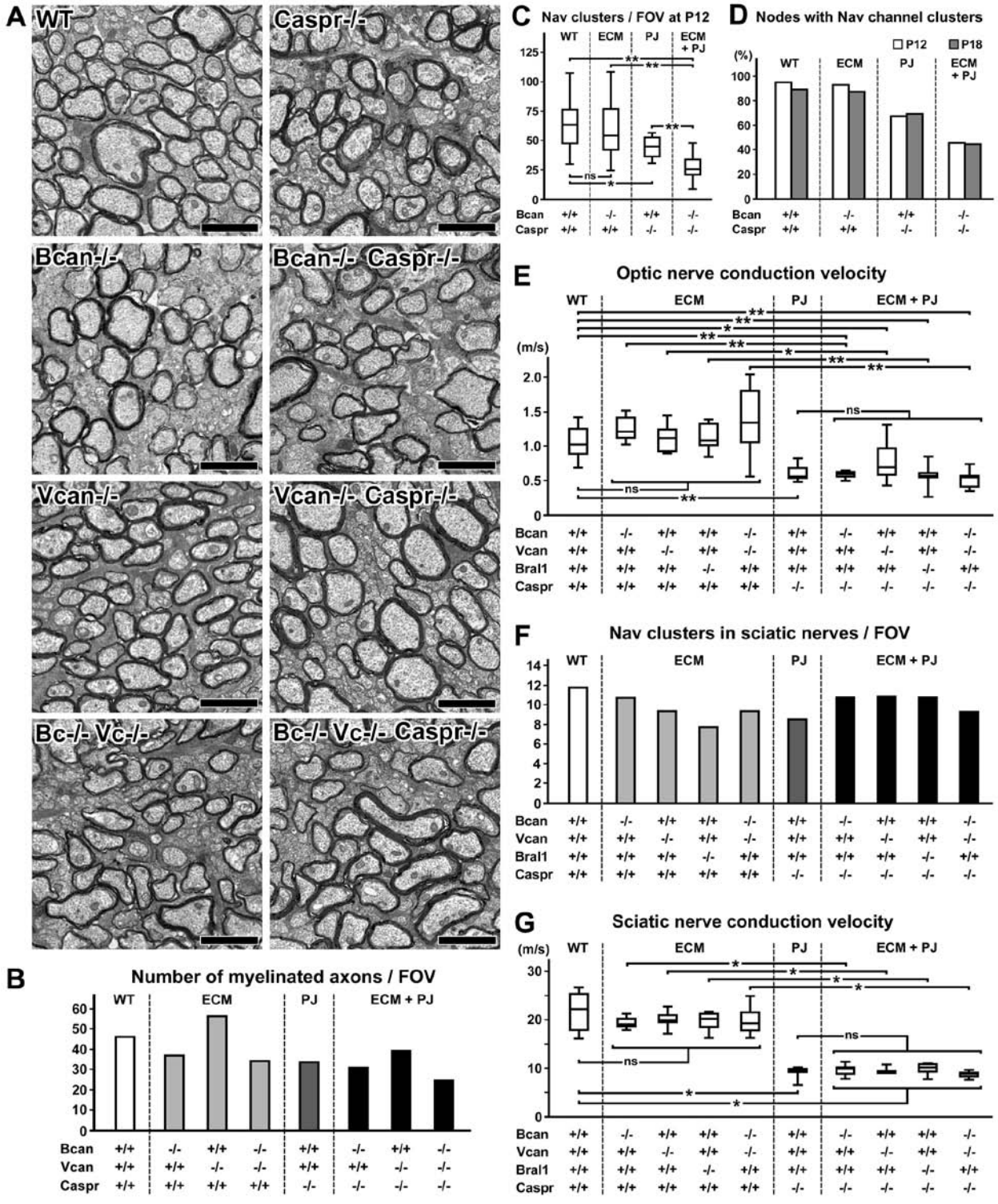
A
WT
Caspr-/-
Bcan-/-
Bcan-/- Caspr-/-
Vcan-/-
Vcan-/- Caspr-/-
Bc-/- Vc-/-
Bc-/- Vc-/- Caspr-/-
B
Number of myelinated axons / FOV
C
Nav clusters / FOV at P12
D
Nodes with Nav channel clusters
P12
P18
E
Optic nerve conduction velocity
F
Nav clusters in sciatic nerves / FOV
G
Sciatic nerve conduction velocity
WT
ECM
PJ
ECM + PJ
Bcan
Vcan
Bral1
Caspr

Figure S2 Legend

Myelination, axon integrity, node formation, and electrophysiology in mutant mice with disrupted ECM and paranodes, related to Figure 4.

(A) Representative electron microscopy images from P18 transverse optic nerve sections. The genotype of each animal is indicated. Scale bars = 2 μm.

(B) The number of myelinated axons per field of view (FOV) (depicted in panel A) in the P18 transverse optic nerve sections. Two to four animals in each genotype were used for the analyses. The mean values are shown from 10 fields per animal.

(C) Quantitation of the number of Na+ channel clusters per FOV at P12 optic nerves from WT (n=2), Bcan-/- (n=3), Caspr-/- (n=2), and Bcan-/- Caspr-/- (n=3) mutants. Data are collected from 10 fields per animal.

(D) The frequency of Na+ channel clusters at nodes in P12 (white bar) or P18 (gray bar) spinal cords. More than 200 nodes (defined by two claudin-11 labeled paranodes) were observed in spinal cords from two animals in each group. Data at P18 are reproduced from Figure 4G.

(E) CAP conduction velocities measured from optic nerves at P18. No significant difference was observed between PJ (Caspr-/-) and ECM+PJ mutants.

(F) The number of Na+ channel clusters per FOV in the sciatic nerves of P18 WT and mutant mice. The mean values are shown from 11-31 fields from two animals in each group.

(G) Motor nerve conduction velocity at P18 sciatic nerves. Note that no significant difference was observed between PJ (Caspr-/-) and ECM+PJ mutants.

WT, wild type; ECM, mutant mice lacking one or two ECM molecules; PJ, Caspr-/- mice lacking paranodal junctions. * = $p<0.01$, ** = $p<0.001$, and ns = not significant.

Figure S3

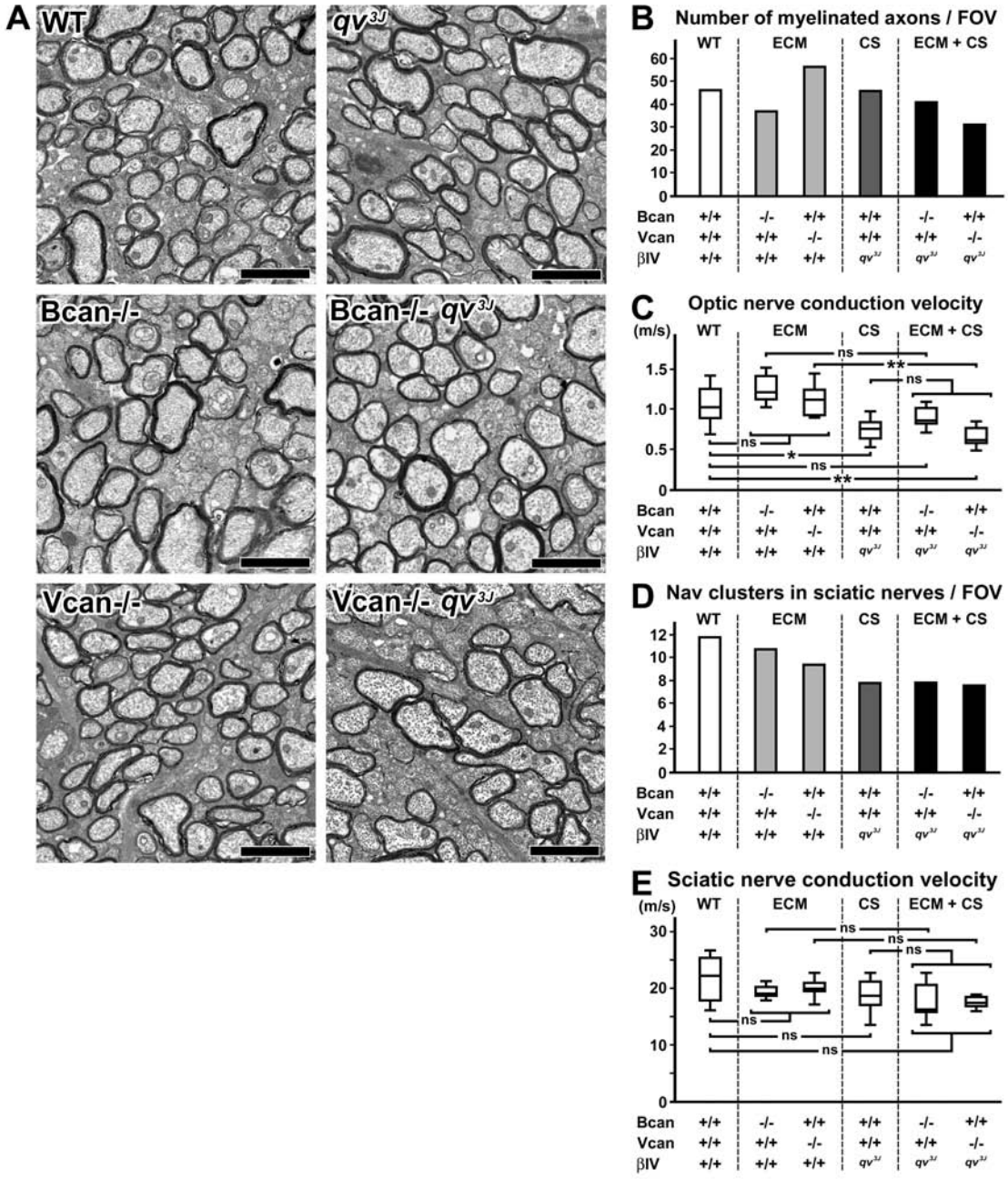
A
WT
qv3J
Bcan-/-
Bcan-/- qv3J
Vcan-/-
Vcan-/- qv3J
B
Number of myelinated axons / FOV
WT
ECM
CS
ECM + CS
60
50
40
30
20
10
0
Bcan +/+ -/- +/+ +/+ -/- +/+
Vcan +/+ +/+ -/- +/+ +/+ -/-
βIV +/+ +/+ +/+ qv3J qv3J qv3J
C
Optic nerve conduction velocity
(m/s)
1.5
1.0
0.5
0
ns
**
ns
ns
*
ns
**
D
Nav clusters in sciatic nerves / FOV
12
10
8
6
4
2
0
E
Sciatic nerve conduction velocity
30
20
10
0
ns
ns
ns
ns
ns
ns

Figure S3 Legend

Myelination, axon integrity, and electrophysiology in mutant mice with disrupted ECM and nodal cytoskeleton, related to Figure 5.

(A) Representative electron microscopy images from P18 transverse optic nerve sections. The genotype of each animal is indicated. Scale bars = 2 μm.

(B) The number of myelinated axons per field of view (FOV) (depicted in panel A) in the P18 transverse optic nerve sections. The mean values are shown from 20 fields from two animals in each group.

(C) CAP conduction velocities measured from optic nerves at P18. No significant difference was observed between CS (*qv3J*) and ECM+CS mutants.

(D) The number of Na+ channel clusters per field of view (FOV) in the sciatic nerves of P18 WT and mutant mice. The mean values are shown from 23-33 fields from two animals in each group.

(F) No significant difference in motor nerve conduction velocity was observed at P18 among the various genotypes.

WT, wild type; ECM, mutant mice lacking a single ECM molecule; CS, *qv3J* mice lacking nodal βIV spectrin. * = $p<0.01$, ** = $p<0.001$, and ns = not significant.

Figure S4

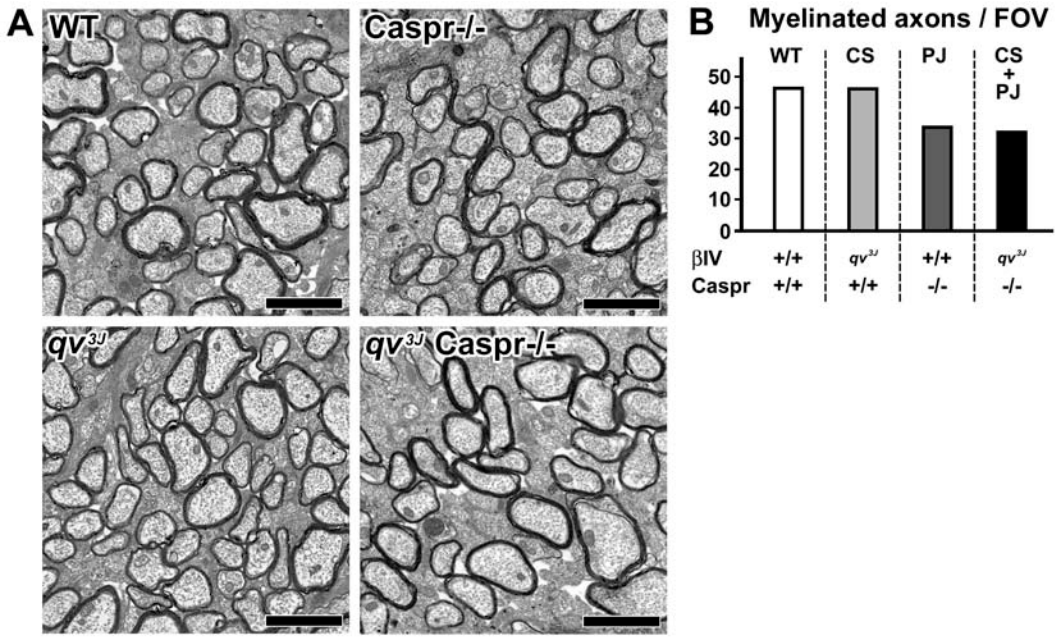

Figure S4 Legend

Myelination and axon integrity in mutant mice with disrupted paranodes and nodal cytoskeleton, related to Figure 6.

(A) Representative electron microscopy images from P18 transverse optic nerve sections. The genotype of each animal is indicated. Scale bars = 2 μm.

(B) The number of myelinated axons per field of view (FOV) (depicted in panel A) in the P18 transverse optic nerve sections. The mean values are shown from 20 fields from two animals in each group.

WT, wild type; CS, *qv3J* mice lacking nodal βIV spectrin; PJ, Caspr-/- mice lacking paranodal junctions.

Table S1, related to Figure 2.

Binding of ECM molecules to nodal membrane proteins in cell surface binding assay

		Brevican			Versican V2				
	Fc	Full	G1	G3	Full	G1	G3	Bral1	NrCAM
NF186[a]	-	+[1]	-	+	-	-	+	+	+[2]
Contactin[b]	-	-	-	-	-	-	-	-	+[3]
Navβ1[c]	-	-	-	-	-	-	-	-	-
Navβ2[d]	-	-	-	-	-	-	+	+	-
Navβ4[e]	-	-	-	-	-	-	-	-	-
NrCAM	-	-	-	-	-	-	-	-	-

[a]Davis et al., 1996
[b]Rios et al., 2000
[c]Ratcliffe et al., 2001
[d]Kaplan et al., 2001
[e]Buffington and Rasband, 2013
[1]as shown in Hedstrom et al., 2007
[2]as shown in Volkmer et al., 1996
[3]as shown in Morales et al., 1993

Supplemental movies

Movie S1 Legend

Brevican-/- Versican-/- Caspr-/- triple mutant and littermate at postnatal day 18, related to Figure 4.

Movie S2 Legend

Brevican-/- *qv3J* double mutant and littermate at postnatal day 18, related to Figure 5.

Movie S3 Legend

Caspr-/- *qv3J* double mutant at postnatal day 18, related to Figure 6.

Supplemental Experimental Procedures

Antibodies. The following primary antibodies were used: mouse monoclonal antibodies to Bcan (N294A/10, UC Davis/NIH NeuroMab Facility) raised against GST-rat Bcan purified from BL21 transformed with pGEX-3X-Bcan (Seidenbecher et al., 1995), Caspr (K65/35, NeuroMab), contactin (K73/20, NeuroMab), pan Nav channel (K58/35; Rasband et al., 1999), rat neurofascin (A12/18, NeuroMab), ankG (N106/36, NeuroMab), actin (C4, EMD Millipore), Kv1.2 (K14/16, NeuroMab), HA (16B12, Covance), Flag (M2, Sigma-Aldrich), and V5 (SV5-Pk1, AbD Serotec); rabbit polyclonal antibodies to Vcan V0/V2 (Dours-Zimmermann et al., 2009), Bral1 (Bekku et al., 2010), NrCAM (ab24344, Abcam), Caspr (Schafer et al., 2004), Nav1.6 (Schafer et al., 2006), βIV spectrin SD and βIV spectrin N-terminal (Yang et al., 2004), ankG antibodies were generated against a C-terminal fusion protein and then affinity purified, claudin11 (Life Technologies), GFP (Life Technologies), and neurofilament M (EMD Millipore); chicken antibodies to neurofascin (R&D Systems), and βIV spectrin SD (Chang et al., 2010); sheep anti-Ncan (R&D Systems); rat anti-GFP (Nacalai USA); guinea pig anti-Bcan (Seidenbecher et al., 1995). Secondary antibodies and Hoechst were from Life Technologies, Jackson ImmunoResearch and Sigma-Aldrich.

***Immunofluorescence studies*.** The optic nerves, brains, spinal cords, and sciatic nerves were rapidly dissected out after killing mice or rats by inhalation of isoflurane (aged >10 days) or by rapid decapitation (aged ≤10 days). The tissues were fixed in 4% paraformaldehyde in 0.1 M PB for 30 min (nerves) or 1 hr (spinal cords), immersed into 20% sucrose in 0.1M PB at 4 ºC overnight, and then embedded in OCT compound. To fix mouse brains, the animals were perfused transcardially with 4% paraformaldehyde followed by post-fixation with the same

fixative for 1 hour. Sections of 20 μm (brains and spinal cords), 16 μm (sciatic nerves and spinal cords), or 10 μm (optic nerves) were cut by microtome or cryostat, and mounted on gelatin-coated coverslips. Cells seeded on coverslips were washed with PBS, fixed in 4% paraformaldehyde in 0.1 M PB for 20 min, and then washed with PBS. Immunostaining of nerve tissues and cells was performed as described previously (Schafer et al., 2004). To calculate the node/paranode ratio of GFP signals in the brains introduced with NF186-GFP constructs, the signal intensity was measured in multiple points (at least 5, depending on the cluster length) at nodes (defined by colocalization of βIV spectrin) and adjacent paranode (defined by colocalization of Caspr), and the average value was used.

DNA constructs. pcDNA3-rat NrCAM cDNA corresponding to D3ZXM9 in UniProt was a gift from Dr. Vann Bennett (Duke University). HA-NrCAM was made by inserting the HA tag between amino acids 32 and 33 of rat NrCAM. NrCAM-EGFP was constructed by replacing the stop codon TAA with CCACCGGTCTAAGCGGCCGC and inserting *Age*I-EGFP-*Not*I from pEGFP-N1 (Clontech). NrCAM(RA) mutants were made by mutating R878 to A; NrCAMΔAC mutants were made by deleting 1039PPDVGAGKAMASRQVD1054. HA-rat NF186 was kindly provided by Dr. Stephen Lambert (University of Central Florida). Rat NF186 was inserted into pCX-EGFP to make NF186-GFP fusion; the various domain deletions were made as depicted in Figure 1A. pCX-CD4-EGFP was described previously (Gasser et al., 2012). To construct Fc-tagged ECM components, the DNA fragments encoding the following regions were inserted into the cloning sites between the mouse Igκ signal peptide and human IgG1 Fc in pSX-Fc (Eshed et al., 2005): amino acids (aa) 25-379 and 615-883 of NP_001028837.1 for rat Bcan G1 and G3, respectively; aa 21-357 and 1328-1642 of AAA67565.1 for human Vcan G1 and G3,

respectively; aa 28-341 of NP_071314.1 for mouse Bral1. Bcan-Fc and Vcan V2-Fc were described previously (Chang et al., 2010). Mouse NrCAM-Fc (Lustig et al., 2001) was a gift from Dr. Martin Grumet (Rutgers University). GldnECD-Fc and GldnOLF-Fc were described previously (Eshed et al., 2005). The open reading frame containing the signal peptide-HA-NF186 whole extracellular domain from the HA-rat NF186 construct was subcloned into pCXMCS to express secreted HA-NF186 extracellular domain (HA-NF186ECD); pCXMCS was constructed by replacing EGFP of pCX-EGFP with a multiple cloning site. Flag-Bral1 was constructed by fusing aa 22-341 of mouse Bral1 downstream to the BM40 signal peptide-Flag and inserting into pCAGGS. pcDNA3.1/GS-human SCN1B and SCN2B were purchased from Life Technologies. Contactin cDNA was a gift from Dr. Barbara Ranscht (The Burnham Institute, La Jolla, CA). pEGFP-N1-SCN4B was constructed by inserting rat SCN4B cDNA into pEGFP-N1. pENTR-AnkG shRNA-CAG-EGFP, pENTR-NF shRNA-CAG-EGFP and pSUPER-NrCAM shRNA were described previously (Hedstrom et al., 2007) and NrCAM shRNA was subcloned into pENTR-CAG-EGFP.

***Analysis of NrCAM shedding*.** The HA-NF186 and various NrCAM constructs were transfected into COS-7 cells in 6-well plates with Lipofectamine 2000 according to the manufacturer's instruction. One day after transfection, the media were changed to 2 ml of fresh regular culture media (DMEM high glucose (Life Technologies) supplemented with 1 X GlutaMAX-I (Life Technologies) and 10% (v/v) FetalClone III (Thermo Scientific)). Two days later, the media were harvested by centrifuging at 3000 X g for 3 min and collecting the supernatants. The cells were collected by scraping in 1 ml of DPBS without calcium and magnesium (Mediatech) on ice and pelleting at 3000 X g for 3 min. For the inhibitor-treated

COS-7 cells, DMSO, 50 μM dec-RVKR-CMK or 50-100 μM GM6001 (both from EMD Millipore) was included while transfection and medium change; the media and cells were collected one day after medium change. Rat hippocampal neurons were treated with DMSO, 50 μM dec-RVKR-CMK or GM6001 at 3 DIV (days *in vitro*) and the media and cells were collected at 6 DIV. For mass spectrometry sequencing, one day after transfection of COS-7 cells with HA-NrCAM(RA) in a 10-cm dish, the medium was changed to VP-SFM (Life Technologies) supplemented with 2 X GlutaMAX-I, collected 2 days later, neutralized by adding 7-8 mM Tris-HCl pH8.0 and concentrated with a Pierce Protein Concentrator (9K MWCO, Thermo Scientific). The secreted HA-NrCAM(RA) fragment was purified by immunoprecipitation with the mouse anti-HA antibody and subjected to SDS-PAGE and Coomassie Blue staining. The band was excised, digested with trypsin and analyzed by mass spectrometry as described previously (Ogawa et al., 2010). The most C-terminal peptide identified not ending in K or R was 1035AGILPPDVGAGKA1047.

***Hippocampal neuron culture and shRNA knockdown*.** Details of primary hippocampal neuron cultures and knockdown of proteins by shRNA can be found in the supplemental procedures. were prepared as described previously (Ogawa et al., 2006). Neurons were plated at a density of 500 cells/mm^2 in 6-well plates to observe Vcan enriched at the AIS. Cells were transfected by adding 2 μg of pENTR-shRNA-CAG-EGFP constructs plus 3 μl of Lipofectamine 2000 in 200 μl of Neurobasal and incubating for 4 hr, then washed twice with 1 ml of warm Neurobasal and returned to the culture medium (Neurobasal supplemented with 1 X GlutaMAX-I and 1 X B-27 Supplement). Cultures at 15-20 DIV were analyzed by immunostaining.

Supplemental References

Bekku, Y., Vargova, L., Goto, Y., Vorisek, I., Dmytrenko, L., Narasaki, M., Ohtsuka, A., Fassler, R., Ninomiya, Y., Sykova, E., and Oohashi, T. (2010). Bral1: its role in diffusion barrier formation and conduction velocity in the CNS. J Neurosci *30*, 3113-3123.

Buffington, S. A., Rasband, M. N. (2013). Na^+ channel-dependent recruitment of $Na_v\beta4$ to axon initial segments and nodes of Ranvier. J Neurosci, *33*, 6191-202.

Chang, K. J., Susuki, K., Dours-Zimmermann, M. T., Zimmermann, D. R., and Rasband, M. N. (2010). Oligodendrocyte myelin glycoprotein does not influence node of ranvier structure or assembly. J Neurosci *30*, 14476-14481.

Davis, J. Q., Lambert, S., and Bennett, V. (1996). Molecular composition of the node of Ranvier: identification of ankyrin-binding cell adhesion molecules neurofascin (mucin+/third FNIII domain-) and NrCAM at nodal axon segments. J Cell Biology *135*, 1355-1367.

Dours-Zimmermann, M. T., Maurer, K., Rauch, U., Stoffel, W., Fassler, R., and Zimmermann, D. R. (2009). Versican V2 assembles the extracellular matrix surrounding the nodes of Ranvier in the central nervous system. Journal of Neuroscience *29*, 7731-7742.

Eshed, Y., Feinberg, K., Poliak, S., Sabanay, H., Sarig-Nadir, O., Spiegel, I., Bermingham, J. R., Jr., and Peles, E. (2005). Gliomedin mediates schwann cell-axon interaction and the molecular assembly of the nodes of ranvier. Neuron *47*, 215-229.

Eshed, Y., Feinberg, K., Carey, D. J., and Peles, E. (2007). Secreted gliomedin is a perinodal matrix component of peripheral nerves. J Cell Biol *177*, 551-562.

Hedstrom, K. L., Xu, X., Ogawa, Y., Frischknecht, R., Seidenbecher, C. I., Shrager, P., and Rasband, M. N. (2007). Neurofascin assembles a specialized extracellular matrix at the axon initial segment. J Cell Biol *178*, 875-886.

Kayyem, J. F., Roman, J. M., de la Rosa, E. J., Schwarz, U., and Dreyer, W. J. (1992). Bravo/Nr-CAM is closely related to the cell adhesion molecules L1 and Ng-CAM and has a similar heterodimer structure. J Cell Biol *118*, 1259-1270.

Lustig, M., Zanazzi, G., Sakurai, T., Blanco, C., Levinson, S. R., Lambert, S., Grumet, M., and Salzer, J. L. (2001). Nr-CAM and neurofascin interactions regulate ankyrin G and sodium channel clustering at the node of Ranvier. Curr Biol *11*, 1864-1869.

Ogawa, Y., Schafer, D. P., Horresh, I., Bar, V., Hales, K., Yang, Y., Susuki, K., Peles, E., Stankewich, M. C., and Rasband, M. N. (2006). Spectrins and ankyrinB constitute a specialized paranodal cytoskeleton. J Neurosci *26*, 5230-5239.

Ogawa, Y., Oses-Prieto, J., Kim, M. Y., Horresh, I., Peles, E., Burlingame, A. L., Trimmer, J. S., Meijer, D., and Rasband, M. N. (2010). ADAM22, a Kv1 channel-interacting protein, recruits membrane-associated guanylate kinases to juxtaparanodes of myelinated axons. J Neurosci *30*, 1038-1048.

Rasband, M. N., Peles, E., Trimmer, J. S., Levinson, S. R., Lux, S. E., and Shrager, P. (1999). Dependence of nodal sodium channel clustering on paranodal axoglial contact in the developing CNS. Journal of Neuroscience *19*, 7516-7528.

Schafer, D. P., Bansal, R., Hedstrom, K. L., Pfeiffer, S. E., and Rasband, M. N. (2004). Does paranode formation and maintenance require partitioning of neurofascin 155 into lipid rafts? J Neurosci *24*, 3176-3185.

Schafer, D. P., Custer, A. W., Shrager, P., and Rasband, M. N. (2006). Early events in node of Ranvier formation during myelination and remyelination in the PNS. Neuron Glia Biol *2*, 69-79.

Seals, D. F., and Courtneidge, S. A. (2003). The ADAMs family of metalloproteases: multidomain proteins with multiple functions. Genes Dev *17*, 7-30.

Seidenbecher, C. I., Richter, K., Rauch, U., Fassler, R., Garner, C. C., and Gundelfinger, E. D. (1995). Brevican, a chondroitin sulfate proteoglycan of rat brain, occurs as secreted and cell surface glycosylphosphatidylinositol-anchored isoforms. J Biol Chem *270*, 27206-27212.

White, J. M. (2003). ADAMs: modulators of cell-cell and cell-matrix interactions. Curr Opin Cell Biol *15*, 598-606.

Yang, Y., Lacas-Gervais, S., Morest, D. K., Solimena, M., and Rasband, M. N. (2004). BetaIV spectrins are essential for membrane stability and the molecular organization of nodes of Ranvier. J Neurosci *24*, 7230-7240.

Zonta, B., Tait, S., Melrose, S., Anderson, H., Harroch, S., Higginson, J., Sherman, D. L., and Brophy, P. J. (2008). Glial and neuronal isoforms of Neurofascin have distinct roles in the assembly of nodes of Ranvier in the central nervous system. J Cell Biol *181*, 1169-1177.